# Recurrent emergence and transmission of a SARS-CoV-2 Spike deletion ΔH69/V70

Kemp SA[1], Datir RP[1], Collier DA[1], Ferreira IATM[2,3], Carabelli A[3], Harvey W[5], Robertson DL[4], Gupta RK[2,3]

[1]Division of Infection and Immunity, University College London, London, UK.
[2]Cambridge Institute of Therapeutic Immunology & Infectious Disease (CITIID), Cambridge, UK.
[3]Department of Medicine, University of Cambridge, Cambridge, UK.
[4] MRC - University of Glasgow Centre for Virus Research, Glasgow, UK.
[5]Institute of Biodiversity, Animal Health and Comparative Medicine, University of Glasgow, Glasgow, UK

Address for correspondence:
Ravindra K. Gupta
Cambridge Institute for Therapeutic Immunology and Infectious Diseases
Jeffrey Cheah Biomedical Centre
Puddicombe Way
Cambridge CB2 0AW, UK
Tel: +44 1223 331491
rkg20@cam.ac.uk

Key words: SARS-CoV-2; COVID-19; antibody escape; neutralising antibodies; mutation; evasion; resistance; fitness; evolution

**Abstract**

SARS-CoV-2 Spike amino acid replacements occur relatively frequently in the receptor binding domain (RBD) and some have a consequences for immune recognition. Here we report recurrent emergence and significant onward transmission of a six nucleotide deletion in the Spike gene, which results in the loss of two amino acids: **Δ**H69/V70. Of particular note this deletion often follows the receptor binding motif amino acid replacements N501Y, N439K and Y453F. In addition, we report a sub-lineage of over 350 sequences bearing seven spike mutations across the RBD (N501Y, A570D), S1 (**Δ**H69/V70) and S2 (P681H, T716I, S982A and D1118H) in England. These mutations have possibly arisen as a result of the virus evolving from immune selection pressure in infected individuals. Enhanced surveillance for the **Δ**H69/V70 deletion with and without RBD mutations should be considered as a priority.

**Background**

SARS-CoV-2's Spike surface glycoprotein engagement of ACE2 is essential for virus entry and infection[1], and the receptor is found in respiratory and gastrointestinal tracts[2]. Despite this critical interaction and related mutational constraints, it appears the RBD can tolerate mutations in this region[3,4], raising the real possibility of virus escape from vaccines and monoclonal antibodies. Spike mutants exhibiting reduced susceptibility to monoclonal antibodies have been identified in *in vitro* screens[5,6]. Some of these have been found in clinical isolates[7]. The unprecedented scale of whole genome SARS-CoV-2 sequencing has enabled identification and epidemiological analysis of transmission. As of December 11$^{th,}$ there were 246,534 SARS-CoV-2 sequences available in the GISAID initiative (https:gisaid.org/).

We recently documented *de novo* emergence of antibody escape mediated by Spike in an individual treated with convalescent plasma (CP), on the background of D614G[8]. Similarly, deletions in the NTD have been reported to provide escape for N-Terminal Domain-specific neutralising antibodies[11]. Dynamic changes in prevalence of Spike variants **Δ**H69/V70 (an out of frame deletion) and D796H variant followed repeated use of CP, and *in vitro* the mutant displayed reduced susceptibility to the CP and multiple other sera, whilst retaining infectivity comparable to wild type[8]. We hypothesised that Spike **Δ**H69/V70 arises either as a compensatory change or as an antibody evasion mechanism as suggested for other NTD

deletions[1], and therefore aimed to characterise specific circumstances around emergence of ΔH69/V70 globally. Here we analysed the publicly available GISAID database for circulating SARS-CoV-2 sequences containing ΔH69/V70.

**Results**

The double deletion ΔH69/V70 was present in over 3,000 sequences worldwide (2.5% of the available data) (Figure 1), and largely in Europe from where most of the sequences in GISAID are derived (Table 1). Many are from the UK and Denmark where sequencing rates are high compared to other countries. ΔH69/V70 is observed in multiple different lineages, representing at least three independent acquisitions of the SARS-CoV-2 Spike ΔH69/V70 deletion (Figure 1). The earliest samples with ΔH69/V70 were detected in Thailand and Germany in January and February 2020 respectively. The prevalence has since increased in other countries since August 2020 (Table 1). Further analysis of sequences revealed firstly that single deletions of either 69 or 70 were uncommon and secondly that some lineages of ΔH69/V70 alone were present, as well as ΔH69/V70 in the context of other mutations in Spike, specifically those in the RBD (Figure 1).

The structural impact of the double deletion was predicted by homology modelling of the spike NTD possessing ΔH69/V70 using SWISS-MODEL. The ΔH69/V70 deletion was predicted to alter the conformation of a protruding loop comprising residues 69-76, with the loop being predicted to be pulled in towards the NTD (Fig 2A). In the pre- and post-deletion conformations, the positions of the alpha carbons of residues 67 and 68 are roughly equivalent whereas the position of Ser71 in the post-deletion structure is estimated to have moved by approximately 6.7Å to approximately occupy the position of His69 in the pre-deletion structure. Concurrently, the positions of Gly72, Thr73, Asn74 and Gly75 are predicted to have changed by 6.5Å, 6.5Å, 4.7Å and 1.9Å respectively, with the overall effect of drawing these residues inwards, resulting in a less dramatically protruding loop; the position of Thr76 in the post-deletion model is roughly equivalent to its position in the pre-deletion structure.

We next examined the lineages where Spike mutations in the RBD were identified at high frequency, in particular N439K, recently reported to be expanding in Europe and detected

97 across the world[3] (Figure 3, Supplementary figure 1). N439K appears to have reduced
98 susceptibility to a small subset of monoclonals targeting the RBD, whilst retaining affinity for
99 ACE2 *in vitro*[3]. The proportion of viruses with ΔH69/V70 was very low between April and
100 August 2020 (likely due to low rates of sampling during local and national lockdown
101 procedures) whilst N439K was expanding (Figure 3). However, steep increases in detection
102 of N439K+ ΔH69/V70 began in September and as of November 26th remarkably there were
103 twice as many cumulative sequences with the deletion as compared to the single N439K
104 (Figure 3). The country with the highest proportion of N439K+ ΔH69/V70 versus N439K
105 alone is England; however, in Scotland, where early growth of N439K was high, there is an
106 inverse relationship with 546 versus 177 sequences for N439K and
107 N439K+ΔH69/V70respectively (as of November 26th). This is attributed to an extinct lineage
108 - Y439K first established in Scotland but went extinct alongside several other lineages due to
109 a national lockdown. These differences therefore likely reflect differing epidemic growth
110 characteristics and timings of the two strains.
111
112 The second significant cluster with ΔH69/V70and RBD mutants involves Y453F along with
113 F486L and N501T related to human-mink transmissions in Denmark[9] (Figure 4). This sub-
114 lineage, termed 'Cluster 5' was part of a wider lineage in which the same out of frame
115 deletion (ΔH69/V70) was observed. In N439K lineages, the mutant virus demonstrates
116 reduced susceptibility to sera from recovered COVID-19 patients (https://files.ssi.dk/Mink-
117 cluster-5-short-report_AFO2). The ΔH69/V70 was first detected in the Y453F background on
118 August 24th and thus far appears limited to Danish sequences.
119
120 A third lineage containing the same out of frame deletion ΔH69/V70 has arisen with the
121 RBD mutation N501Y (Figure 5, supplementary figure 2). Based on location it might be
122 expected to escape antibodies similar to COV2-2499[5]. In addition, when SARS-CoV-2 was
123 passaged in mice for adaptation purposes, N501Y emerged and increased pathogenicity[10].
124 Early sequences with N501Y alone were isolated both in Brazil and USA in April 2020. N501Y
125 + ΔH69/V70sequences appear to have been detected first in the UK in September 2020,
126 with the crude cumulative number of N501Y + ΔH69/V70 mutated sequences now
127 exceeding the single mutant (Figure 5). Of particular concern is a sub-lineage of around 350
128 sequences (Figure 6) bearing six spike mutations across the RBD (N501Y, A570D) and S2

(P681H, T716I, S982A and D1118H) as well as the ΔH69/V70 in England (Figure 7). This cluster has a very long branch (Figure 6).

## Discussion

We have presented data demonstrating multiple, independent, and successful lineages of SARS-CoV-2 variants bearing a Spike deletion - ΔH69/V70. This replacement representing a six-nucleotide out-of-frame deletion, has frequently followed receptor binding mutations and prevalence is rising in parts of Europe, with the greatest increases since August 2020. The Spike deletion ΔH69/V70 was found to follow receptor binding mutations such as N501Y, N439K and Y453F which have been shown to reduce binding with monoclonal antibodies.

A recent analysis highlighted the likely transmissibility of viruses with deletions in the N-terminal domain, including ΔH69/V70[11]. The potential for SARS-CoV-2 mutations to rapidly emerge and fix is exemplified by D614G, a mutation in S2 that alters linkages between S1 and S2 subunits on adjacent protomers as well as RBD orientation, infectivity, and transmission[12-14]. The example of D614G also demonstrates that mechanisms directly impacting important biological processes can be indirect. Similarly, a number of possible mechanistic explanations may underlie ΔH69/V70. For example, the fact that it sits on an exposed surface might be suggestive of immune interactions and escape, although allosteric interactions could alternatively lead to higher infectivity.

We are concerned by the finding of a sub-lineage of over 350 sequences bearing seven spike mutations across the RBD (N501Y, A570D), S1 (ΔH69/V70) and S2 (P681H, T716I, S982A and D1118H) in England. The finding of a long branch to this cluster of cases suggests viral evolution may have occurred during a chronic infection.

Given the emergence of significant clusters of viruses carrying RBD mutations and the ΔH69/V70 deletion, limitation of transmission takes on a renewed urgency. Concerted global vaccination efforts with wide coverage should be accelerated. Continued emphasis on testing/tracing, social distancing and mask wearing are essential, with investment in other novel methods to limit transmission[15]. Detection of the deletion by rapid diagnostics

should be a research priority as such tests could be used as a proxy for antibody escape mutations to inform surveillance at global scale.

**Acknowledgements**

RKG is supported by a Wellcome Trust Senior Fellowship in Clinical Science (WT108082AIA). SAK is supported by the Bill and Melinda Gates Foundation via PANGEA grant: OPP1175094. DLR is funded by the MRC (MC UU 1201412). WH is funded by the MRC (MR/R024758/1). We thank Dr James Voss for the kind gift of HeLa cells stably expressing ACE2.

**Conflicts of interest**

RKG has received consulting fees from UMOVIS lab, Gilead Sciences and ViiV Healthcare, and a research grant from InvisiSmart Technologies.

**Methods**

*Phylogenetic Analysis*

All available full-genome SARS-CoV-2 sequences were downloaded from the GISAID database (http://gisaid.org/) [16] on 26th November. Duplicate and low-quality sequences (>5% N regions) were removed, leaving a dataset of 194,265 sequences with a length of >29,000bp.. All sequences were realigned to the SARS-CoV-2 reference strain MN908947.3, using MAFFT v7.473 with automatic flavour selection and the --keeplength --addfragments options[17]. Major SARS-CoV-2 clade memberships were assigned to all sequences using the Nextclade server v0.9 (https://clades.nextstrain.org/).

Maximum likelihood phylogenetic trees were produced using the above curated dataset using IQ-TREE v2.1.2 [18]. Evolutionary model selection for trees were inferred using ModelFinder [19] and trees were estimated using the GTR+F+I model with 1000 ultrafast bootstrap replicates [20]. All trees were visualised with Figtree v.1.4.4 (http://tree.bio.ed.ac.uk/software/figtree/), rooted on the SARS-CoV-2 reference sequence and nodes arranged in descending order. Nodes with bootstraps values of <50 were collapsed using an in-house script.

193

194 *Pseudotype virus preparation*

195 Viral vectors were prepared by transfection of 293T cells by using Fugene HD transfection
196 reagent (Promega). 293T cells were transfected with a mixture of 11ul of Fugene HD, 1µg of
197 pCDNAΔ19Spike-HA, 1ug of p8.91 HIV-1 gag-pol expression vector[22,23], and 1.5µg of pCSFLW
198 (expressing the firefly luciferase reporter gene with the HIV-1 packaging signal). Viral
199 supernatant was collected at 48 and 72h after transfection, filtered through 0.45um filter
200 and stored at -80˚C as previously described[24]. Infectivity was measured by luciferase
201 detection in target TZMBL transduced to express TMPRSS2 and ACE2.

202

203 *Normalisation of virus titre by SG-PERT to measure RT activity in lentivirus preparation*

204 Supernatant was subjected to SG-PERT as previously described.[25]

205

206 *Homology modelling*

207 Prediction of conformational change in the spike N-terminal assessed by homology
208 modelling of the NTD (residues 14-306) predicted by homology modelling using SWISS-
209 MODEL[26] with template chain A of PDB 7C2L[27] and aligned with 7C2L using PyMOL. Figures
210 prepared with PyMOL (Schrödinger) using PDBs 7C2L, 6ZGE28 and 6ZGG[28].

211

212

213 1 Zhou, P. *et al.* A pneumonia outbreak associated with a new coronavirus of probable bat
214 origin. *Nature* 579, 270-273, doi:10.1038/s41586-020-2012-7 (2020).
215 2 Sungnak, W. *et al.* SARS-CoV-2 entry factors are highly expressed in nasal epithelial cells
216 together with innate immune genes. *Nature medicine* 26, 681-687, doi:10.1038/s41591-
217 020-0868-6 (2020).
218 3 Thomson, E. C. *et al.* The circulating SARS-CoV-2 spike variant N439K maintains fitness
219 while evading antibody-mediated immunity. *bioRxiv*, 2020.2011.2004.355842,
220 doi:10.1101/2020.11.04.355842 (2020).
221 4 Starr, T. N. *et al.* Deep Mutational Scanning of SARS-CoV-2 Receptor Binding Domain
222 Reveals Constraints on Folding and ACE2 Binding. *Cell* 182, 1295-1310 e1220,
223 doi:10.1016/j.cell.2020.08.012 (2020).

5 Greaney, A. J. *et al.* Complete Mapping of Mutations to the SARS-CoV-2 Spike Receptor-Binding Domain that Escape Antibody Recognition. *Cell host & microbe*, doi:10.1016/j.chom.2020.11.007 (2020).

6 Starr, T. N. *et al.* Prospective mapping of viral mutations that escape antibodies used to treat COVID-19. *bioRxiv*, doi:10.1101/2020.11.30.405472 (2020).

7 Choi, B. *et al.* Persistence and Evolution of SARS-CoV-2 in an Immunocompromised Host. *N Engl J Med*, doi:10.1056/NEJMc2031364 (2020).

8 Kemp, S. A. *et al.* Neutralising antibodies drive Spike mediated SARS-CoV-2 evasion. *medRxiv*, 2020.2012.2005.20241927, doi:10.1101/2020.12.05.20241927 (2020).

9 Oude Munnink, B. B. *et al.* Transmission of SARS-CoV-2 on mink farms between humans and mink and back to humans. *Science*, doi:10.1126/science.abe5901 (2020).

10 Gu, H. *et al.* Adaptation of SARS-CoV-2 in BALB/c mice for testing vaccine efficacy. *Science* 369, 1603-1607, doi:10.1126/science.abc4730 (2020).

11 McCarthy, K. R. *et al.* Natural deletions in the SARS-CoV-2 spike glycoprotein drive antibody escape. *bioRxiv*, 2020.2011.2019.389916, doi:10.1101/2020.11.19.389916 (2020).

12 Korber, B. *et al.* Tracking Changes in SARS-CoV-2 Spike: Evidence that D614G Increases Infectivity of the COVID-19 Virus. *Cell*, doi:10.1016/j.cell.2020.06.043 (2020).

13 Yurkovetskiy, L. *et al.* Structural and Functional Analysis of the D614G SARS-CoV-2 Spike Protein Variant. *Cell* 183, 739-751 e738, doi:10.1016/j.cell.2020.09.032 (2020).

14 Hou, Y. J. *et al.* SARS-CoV-2 D614G variant exhibits efficient replication ex vivo and transmission in vivo. *Science*, doi:10.1126/science.abe8499 (2020).

15 Mlcochova, P. *et al.* Extended in vitro inactivation of SARS-CoV-2 by titanium dioxide surface coating. *bioRxiv*, 2020.2012.2008.415018, doi:10.1101/2020.12.08.415018 (2020).

16 Shu, Y. & McCauley, J. GISAID: Global initiative on sharing all influenza data - from vision to reality. *Euro surveillance : bulletin Europeen sur les maladies transmissibles = European communicable disease bulletin* 22, 30494, doi:10.2807/1560-7917.ES.2017.22.13.30494 (2017).

17 Katoh, K. & Standley, D. M. MAFFT Multiple Sequence Alignment Software Version 7: Improvements in Performance and Usability. *Molecular Biology and Evolution* 30, 772-780, doi:10.1093/molbev/mst010 (2013).

18 Minh, B. Q. *et al.* IQ-TREE 2: New Models and Efficient Methods for Phylogenetic Inference in the Genomic Era. *Molecular Biology and Evolution* 37, 1530-1534, doi:10.1093/molbev/msaa015 (2020).

19 Kalyaanamoorthy, S., Minh, B. Q., Wong, T. K. F., von Haeseler, A. & Jermiin, L. S. ModelFinder: fast model selection for accurate phylogenetic estimates. *Nature Methods* 14, 587-589, doi:10.1038/nmeth.4285 (2017).

20 Minh, B. Q., Nguyen, M. A. T. & von Haeseler, A. Ultrafast Approximation for Phylogenetic Bootstrap. *Molecular Biology and Evolution* 30, 1188-1195, doi:10.1093/molbev/mst024 (2013).

21 Sagulenko, P., Puller, V. & Neher, R. A. TreeTime: Maximum-likelihood phylodynamic analysis. *Virus evolution* 4, vex042-vex042, doi:10.1093/ve/vex042 (2018).

22 Naldini, L., Blomer, U., Gage, F. H., Trono, D. & Verma, I. M. Efficient transfer, integration, and sustained long-term expression of the transgene in adult rat brains injected with a lentiviral vector. *Proceedings of the National Academy of Sciences of the United States of America* 93, 11382-11388 (1996).

23 Gupta, R. K. *et al.* Full-length HIV-1 Gag determines protease inhibitor susceptibility within in vitro assays. *Aids* 24, 1651-1655, doi:10.1097/QAD.0b013e3283398216 (2010).

24 Mlcochova, P. *et al.* Combined point of care nucleic acid and antibody testing for SARS-CoV-2 following emergence of D614G Spike Variant. *Cell Rep Med*, 100099, doi:10.1016/j.xcrm.2020.100099 (2020).

25 Gregson, J. *et al.* HIV-1 viral load is elevated in individuals with reverse transcriptase mutation M184V/I during virological failure of first line antiretroviral therapy and is associated with compensatory mutation L74I. *The Journal of infectious diseases*, doi:10.1093/infdis/jiz631 (2019).

26 Waterhouse *et al.* SWISS-MODEL: homology modelling of protein structures and complexes. Nucleic Acids Res 46, 296-303, doi:https://doi.org/10.1093/nar/gky427 (2018).

27 Chi *et al.* A neutralizing human antibody binds to the N-terminal domain of the Spike protein of SARS-CoV-2. *Science* 369, 650-655, doi:10.1126/science.abc6952 (2020).

28 Wrobel *et al.* SARS-CoV-2 and bat RaTG13 spike glycoprotein structures inform on virus evolution and furin-cleavage effects. *Nat Struct Mol Biol* 27, 763-767, doi:10.1038/s41594-020-0468-7 (2020).

288

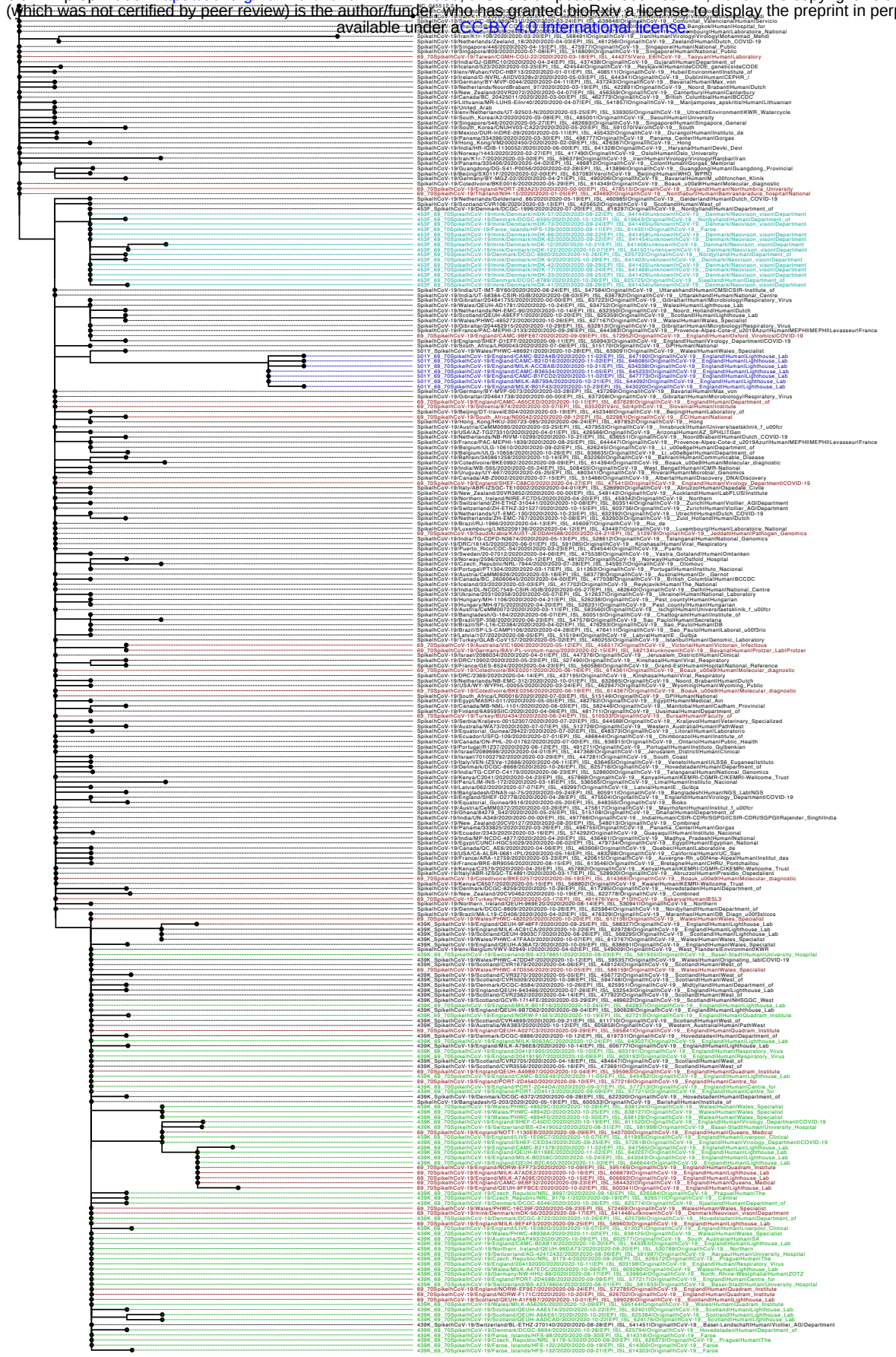

**Figure 1. Global spike-only phylogeny of SARS-CoV-2 sequences carrying the Spike ΔH69/V70 deletion.** All sequences carrying the double-deletion were downloaded from the GISAID database and aligned to the Wuhan-Hu-1 reference strain using MAFFT. A series of global background sequences were also downloaded and used to place mutants into context. All duplicate sequences were removed. The inferred phylogeny suggests that there are multiple lineages of sequences carrying the ΔH69/V70, by itself (red), as well as with RDB mutations N501Y (dark blue), N453F (cyan) and Y439K (green).

| | | Jan | Feb | Mar | Apr | May | Jun | Jul | Aug | Sep | Oct | Nov | Total |
|---|---|---|---|---|---|---|---|---|---|---|---|---|---|
| All ΔH69/V70 and RBD mutations 439K, 453F and 501Y | Australia | | | | | 1 | 1 | | | 1 | 2 | | 5 |
| | Burkina Faso | | | | | | | | 1 | 1 | | | 2 |
| | Canada | | | | | | | | | 1 | | | 1 |
| | Cote d'Ivoire | | | | | | 5 | | | | | | 5 |
| | Czech Republic | | | | | | | | | 12 | 53 | | 65 |
| | Denmark | | | | 1 | | | | **53** | **281** | **611** | **3** | 949 |
| | England | | | | 3 | | | 2 | **184** | **253** | **572** | **449** | 1465 |
| | Faroe Islands | | | | | | | | | 9 | | | 9 |
| | France | | | 1 | | | | | | 9 | | | 10 |
| | Germany | | 1 | | | | | | 1 | 3 | | | 5 |
| | Italy | | | 3 | | | | | | | | | 3 |
| | Malaysia | | | 1 | 1 | | | | | | | | 2 |
| | Netherlands | | | | | | | | | | 9 | | 9 |
| | New Zealand | | | | | | | | 1 | | | | 1 |
| | Northern Ireland | | | | | | | | 20 | 1 | 1 | | 22 |
| | Norway | | | | | | | | | 1 | | | 1 |
| | Saudi Arabia | | | | 1 | | | | | | | | 1 |
| | Scotland | | | | | | | | 25 | 68 | 83 | 2 | 178 |
| | Slovenia | | | 4 | | | | | | | | | 4 |
| | South Africa | | | | | | | 1 | | | | | 1 |
| | Sweden | | | 1 | | | | | | 1 | 1 | | 3 |
| | Switzerland | | | | | | | | 9 | | | | 9 |
| | Taiwan | | | 1 | | | | | | | | | 1 |
| | Thailand | 1 | | | | | | | | | | | 1 |
| | Turkey | | | 2 | | | | | | | | | 2 |
| | USA | | | | 1 | | 1 | | | | | | 2 |
| | Wales | | | | | | | | 14 | 101 | 174 | 20 | 309 |
| | Grand Total | 1 | 1 | 13 | 7 | 1 | 7 | 3 | 308 | 742 | 1506 | 474 | 3065 |
| Only 69/70 (without RBD replacements) | Denmark | | | | | | | | 28 | 109 | 212 | 4 | 353 |
| | Faroe Islands | | | | | | | | | 3 | | | 3 |
| | Turkey | | | | | | 1 | | | | | | 1 |
| | United Kingdom | | | | | | | | 2 | 6 | 6 | | 14 |
| | Grand Total | | | | | | 1 | | 30 | 118 | 218 | 4 | 371 |

**Table 1. Number of reported SARS-CoV-2 sequences with the ΔH69/V70 deletion.** All sequences containing the **Δ**H69/V70 deletion were extracted from the GISAID database (Accessed 26th Nov 2020) and tabulated according to both reporting country of origin and date in which they were posted online. The lineages carrying **Δ**H69/V70 began to expand in both Denmark and England in August 2020.

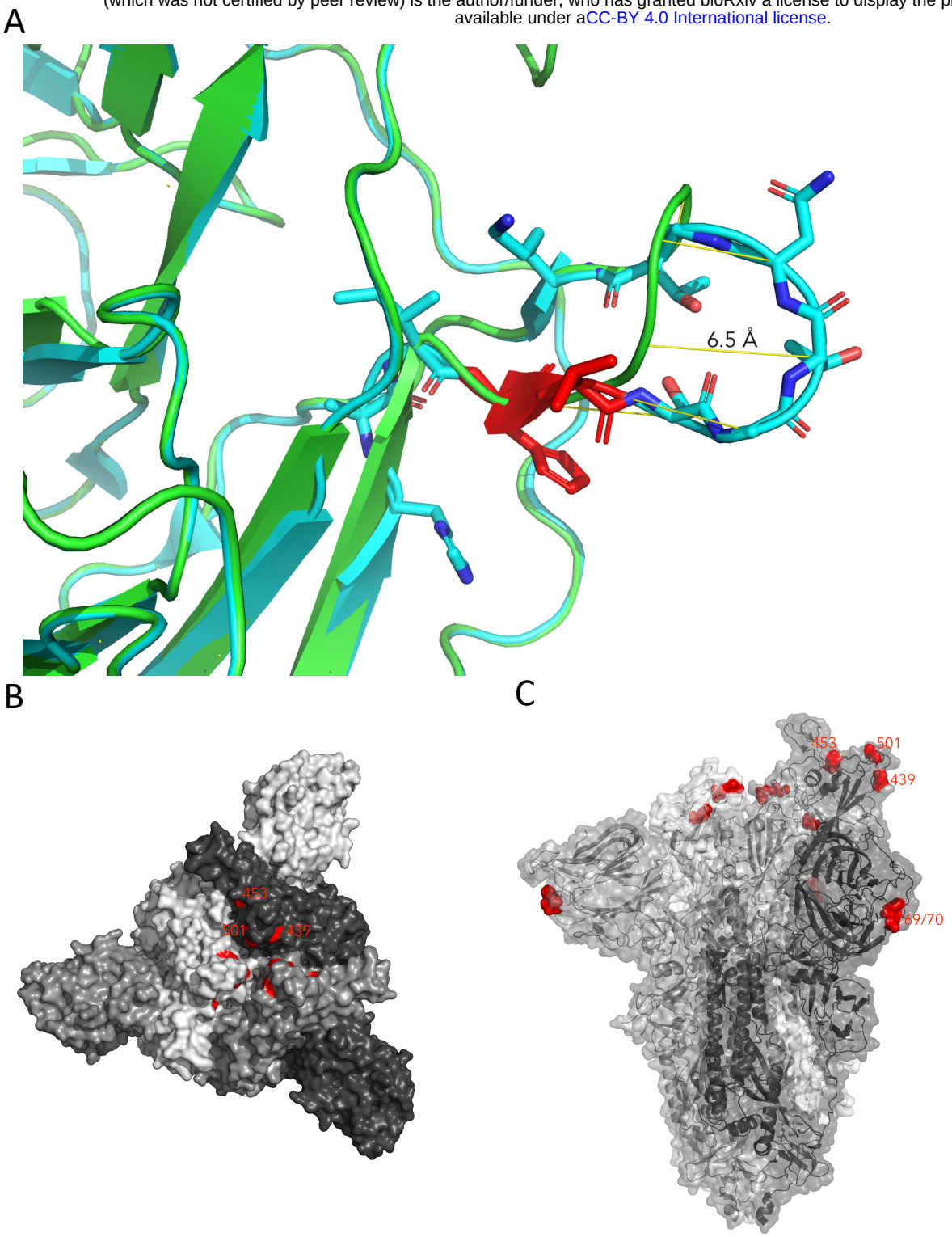


**Figure 2. Structural aspects of ΔH69/V70 A**) Prediction of conformational change in the spike N-terminal domain due to deletion of residues His69 and Val70. The pre-deletion structure is shown in cyan, except for residues 69 and 70, which are shown in red. The predicted post-deletion structure is shown in green. Residues 66-77 of the pre-deletion structure are shown in stick representation and coloured by atom (carbon in cyan, nitrogen in blue, oxygen in coral). Yellow lines connect aligned residues 66-77 of the pre- and post-deletion structures and the distance of 6.5 Å between aligned alpha carbons of Thr73 in the pre- and post-deletion conformation is labelled. **B**) Surface representation of spike homotrimer in closed conformation (PDB: 6ZGE, Wrobel et al., 2020) homotrimer viewed in a 'top-down' view along the trimer axis with each monomer in shown in different shades of grey and locations of RBD mutations at residues 439, 453 and 501 highlighted in red. **C**) Spike in open conformation with a single erect RBD (PDB: 6ZGG, Wrobel et al. 2020) in trimer axis vertical view with the locations of deleted residues His69 and Val70 in the N-terminal domain and RBD mutations highlighted as red spheres and labelled on the monomer with erect RBD. Residues 71-75, which form the exposed loop undergoing conformational change in **A**, are omitted from this structure.

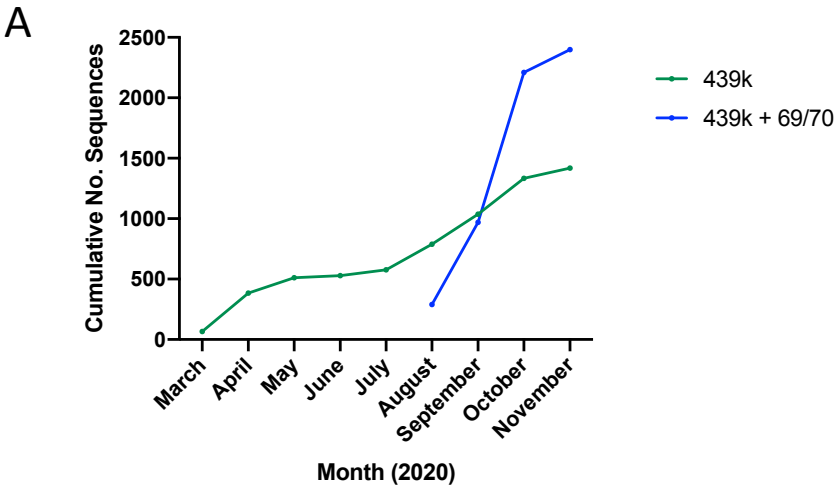


**Figure 3. The relative increase in frequency of sequences bearing Spike mutants 439K and 501Y based on sampling dates.** Between August and October 2020, an exponential increase in mutants carrying both 439K and **Δ**H69/V70 saw the latter become dominant in terms of cumulative cases.

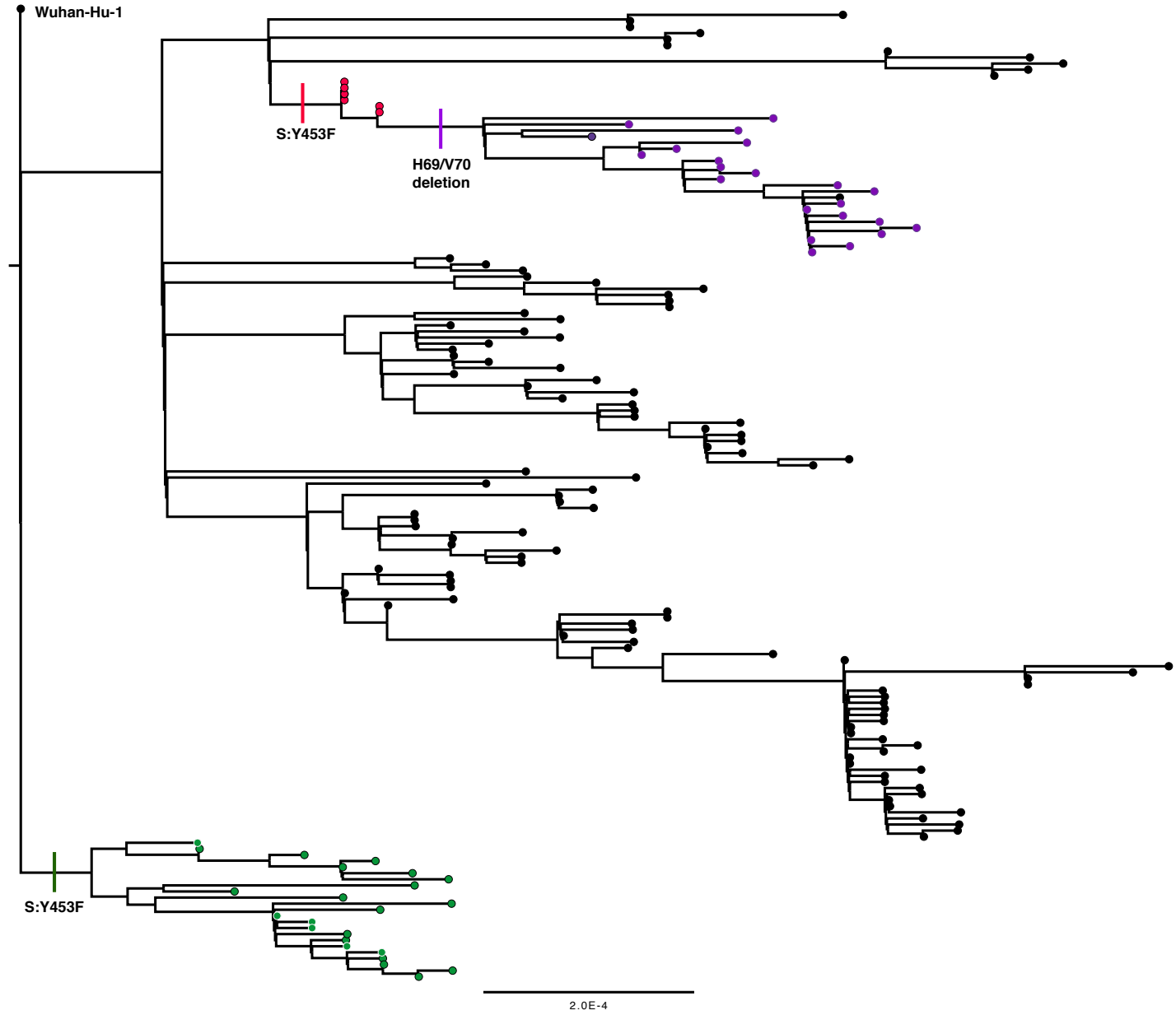


**Figure 4. Maximum likelihood phylogeny of all Mink-origin SARS-CoV-2 Spike sequences.** All 753 publicly available Mink origin Spike sequences were downloaded from the GISAID database (accessed 12th December) and aligned to the Wuhan-Hu-1 reference sequence using MAFFT. Acquisition of the Spike mutant Y453F, an exposed region in the RBD, occurred early on in Dutch Mink (green circles). Later in infection, 453F was acquired by Danish Mink (red) and subsequently, those with the 453F mutant also acquired the **Δ**H69/V70 double deletion (purple).

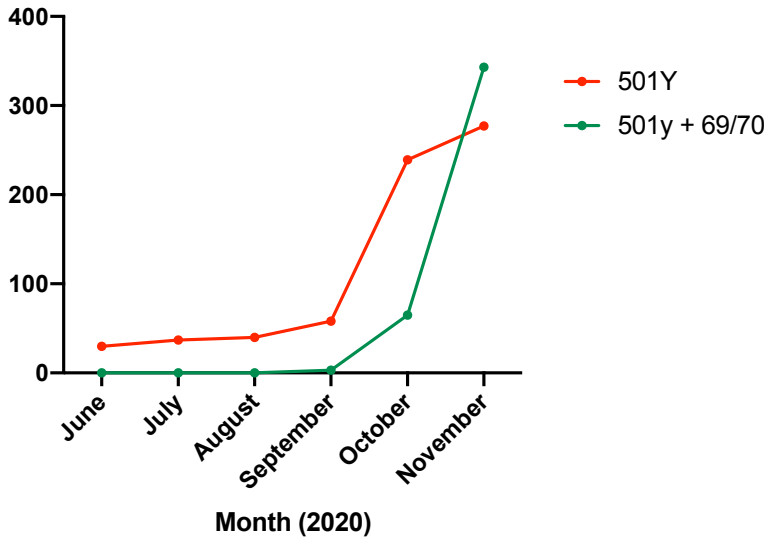


**Figure 5. The relative increase in frequency of sequences bearing Spike mutant 501Y based on sampling dates.** Between October and November 2020, the sequences carrying both 501Y and the **Δ**H69/V70 also became dominant.

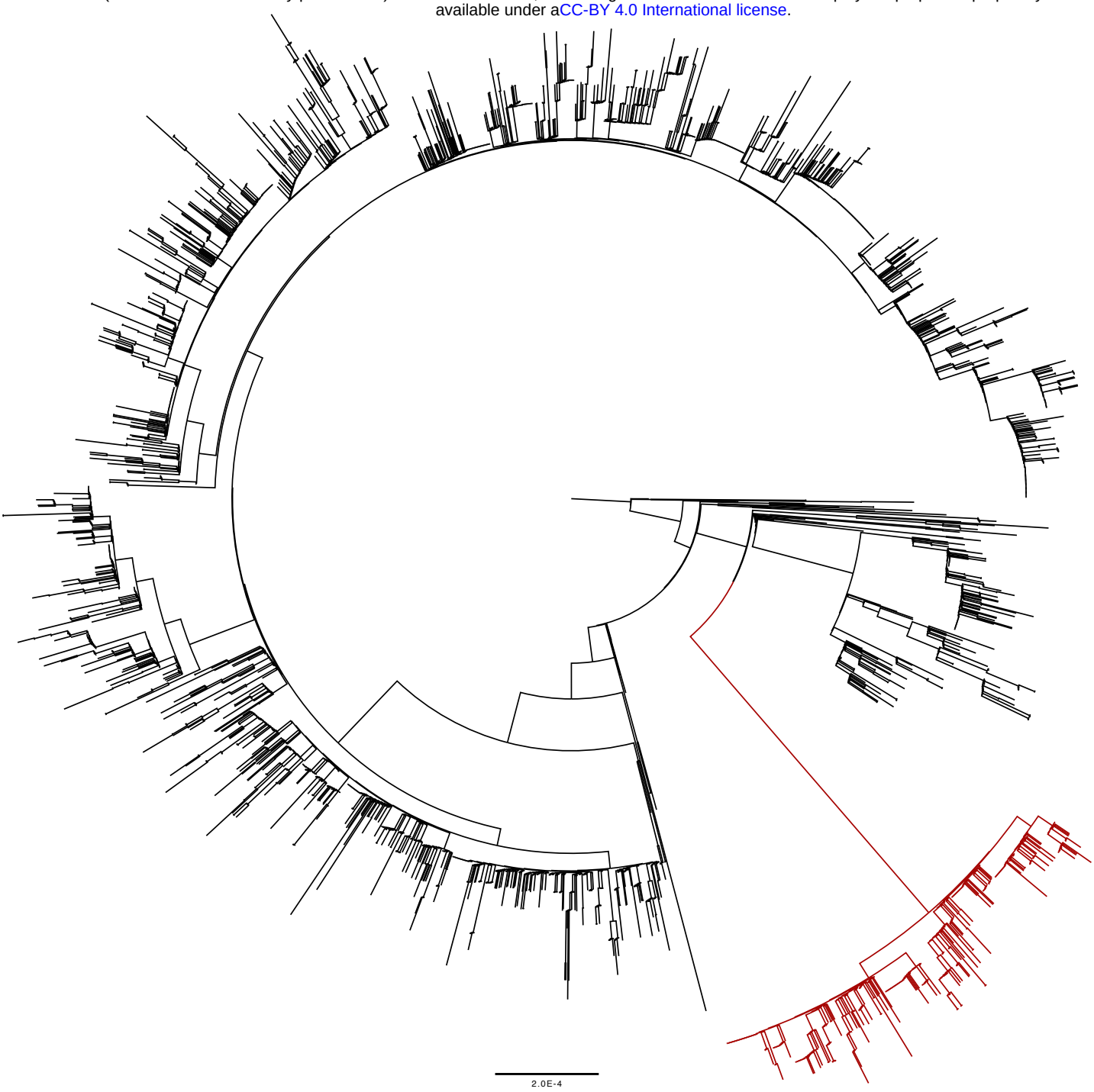


**Figure 6: Lineage bearing multiple Spike mutations including ΔH69/V70:** Global maximum likelihood phylogeny of all ΔH69/V70 sequences downloaded from the GISAID database (3066 sequences, accessed 26th November 2020). A distinct sub-lineage of ΔH69/V70 sequences (red) developed with six linked S mutations, two of which are in the RBD (N501Y and A570D) and four others in S2 (P681H, T716I, S982A and D1118H). All five mutations occur together in all cases with the deletion.

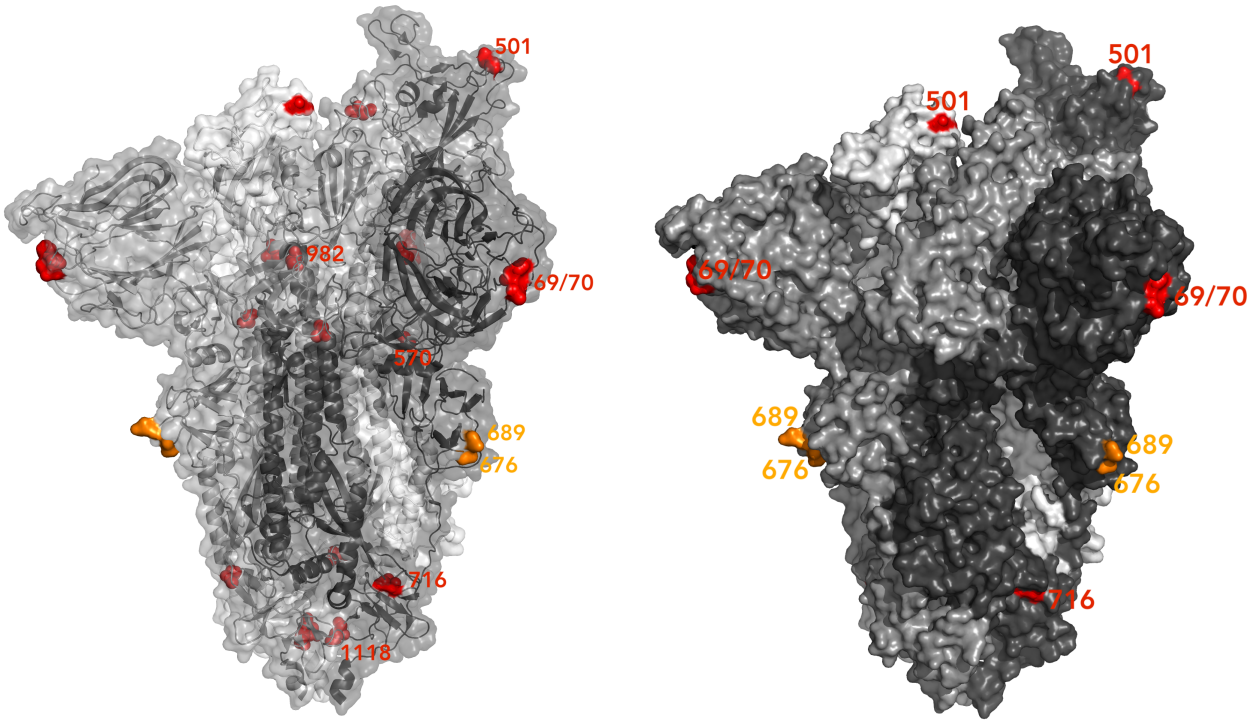


**Figure 7. Spike residues in a highly mutated circulating strain with ΔH69/V70.** Spike homotrimer in open conformation with one upright RBD (PDB: 6ZGE, Wrobel et al., 2020) with different monomers shown in shades of grey. To the left, surface representation overlaid with ribbon representation and to the right, opaque surface representation accentuating the locations of surface-exposed residues. The deleted residues 69 and 70 and the residues involved in amino acid substitutions (501, 570, 716, 982 and 1118) are coloured red. The location of an exposed loop including residue 681 is absent from the structure, though the residues either side of the unmodelled residues, 676 and 689, are coloured orange. On the left structure, highlighted residues are labelled on the monomer with an upright RBD; on the right structure, all visible highlighted residues are labelled.

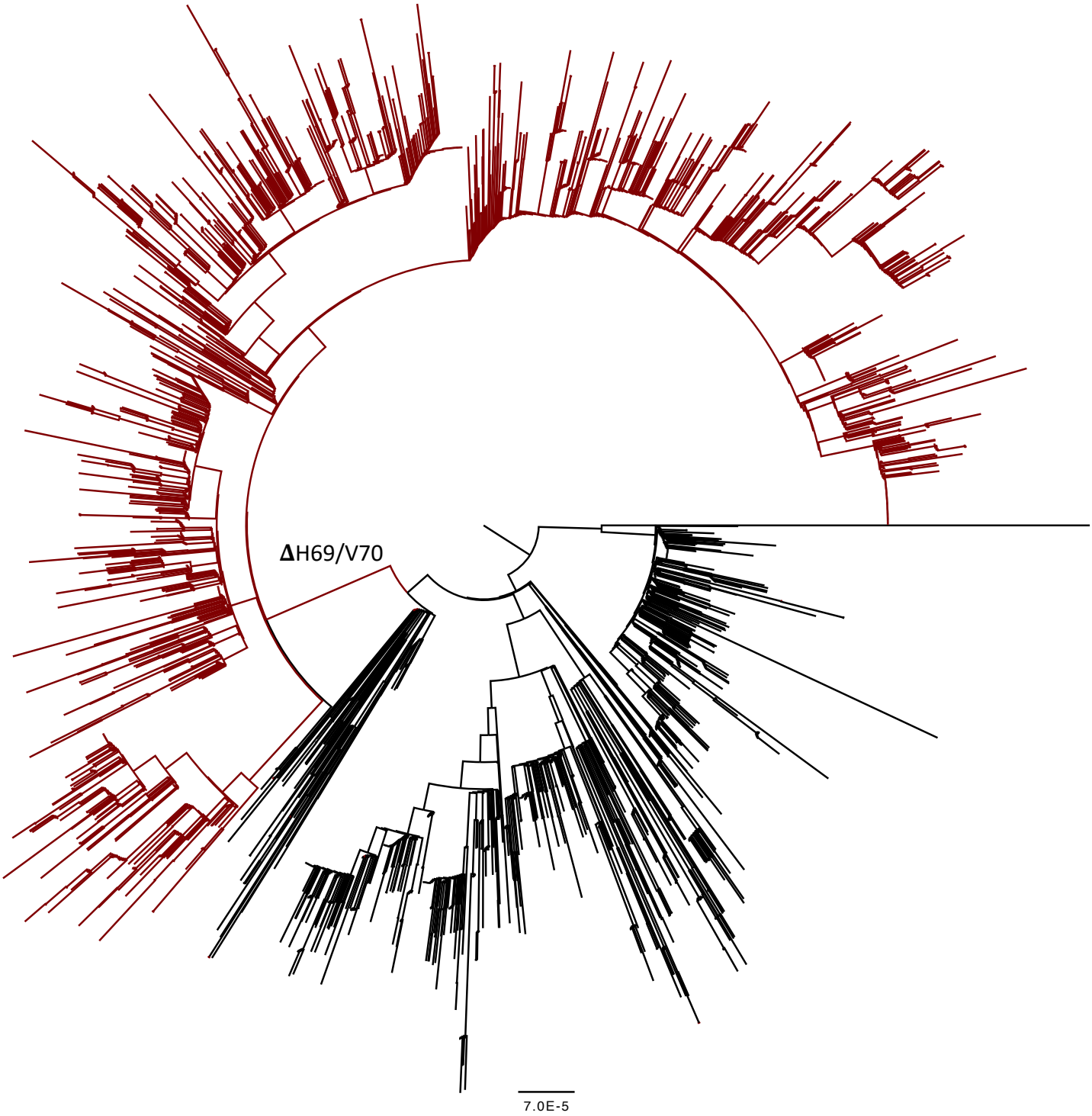


**Supplementary Figure 1. Circularised maximum likelihood phylogeny of global sequences carrying Spike mutant 439K.** All sequences in the GISAID database containing S:439K (3820 sequences, 26th November 2020) were realigned to Wuhan-Hu-1 using MAFFT. Viruses carrying the Spike double deletion **Δ**H69/V70 (red) emerged and expanded from viruses with S:439K (black).

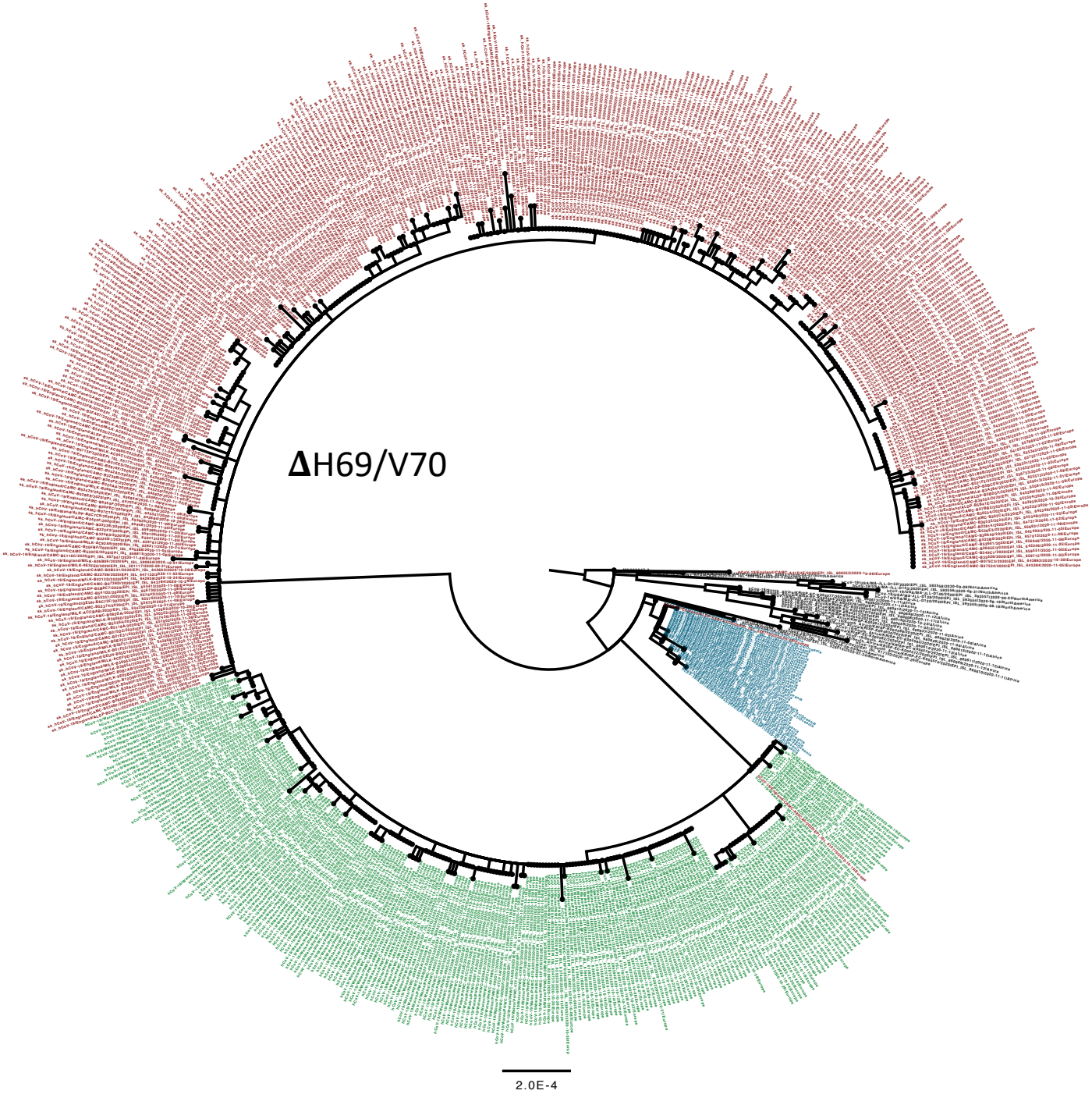


**Supplementary Figure 2. Circularised maximum likelihood phylogeny of global sequences carrying Spike mutant 501Y.** All sequences in the GISAID database containing S:501Y were downloaded and realigned to Wuhan-Hu-1 using MAFFT. Sequences were broadly split into four major clades; sequences carrying the Spike double deletion **Δ**H69/V70 (red) formed an entirely separate clade from non-carriers. Sequences carrying 501Y but an absence of **Δ**H69/V70 formed a second lineage and appeared to expand only in Wales (green). Another major clade (blue) was limited entirely to Australia and finally a fourth clade (black) was limited to several African countries and Brazil.